ARTICLE
Journal of Cellular Biochemistry 116:797–808 (2015)

Journal of Cellular Biochemistry

Reciprocal Modulation of Histone Deacetylase Inhibitors Sodium Butyrate and Trichostatin A on the Energy Metabolism of Breast Cancer Cells

Mariana Figueiredo Rodrigues,[1] Érika Carvalho,[1] Paula Pezzuto,[2] Franklin David Rumjanek,[1] and Nivea Dias Amoêdo[1]*

[1]*Instituto de Bioquímica Médica Leopoldo de Meis, Universidade Federal do Rio de Janeiro, Ilha do Fundão - Rio de Janeiro, Brazil*

[2]*Instituto de Biologia – Departamento de Genética, Universidade Federal do Rio de Janeiro, Ilha do Fundão - Rio de Janeiro, Brazil*

ABSTRACT

Tumor cells display different bioenergetic profiles when compared to normal cells. In the present work we showed metabolic reprogramming by means of inhibitors of histone deacetylase (HDACis), sodium butyrate and trichostatin A in breast cancer cells representing different stages of aggressiveness and metabolic profile. When testing the effect of NaB and TSA on viability of cells, it was shown that non-tumorigenic MCF-10A cells were less affected by increasing doses of the drugs than the tumorigenic, hormone dependent, tightly cohesive MCF-7, T-47D and the highly metastatic triple-negative MDA-MB 231 cells. T-47D cells were the most sensitive to treatment with both, NaB and TSA. Experiments measuring anchorage- independent growth of tumor cells showed that MCF-7, T-47D, and MDA-MB-231 cells were equally sensitive to the treatment with NaB. The NaB induced an attenuation of glycolysis, reflected by a decrease in lactate release in MCF-7 and T47D lines. Pyruvate kinase activity was significantly enhanced by NaB in MDA-MB-231 cells only. In contrast, the inhibitor enhanced lactate dehydrogenase activity specifically in T-47 D cells. Glucose-6-phosphate dehydrogenase activity was shown to be differentially modulated by NaB in the cell lines investigated: the enzyme was inhibited in MCF-7 cells, whereas in T-47D and MDA-MB-231 cells, G6PDH was activated. NaB and TSA were able to significantly increase the oxygen consumption by MDA-MB-231 and T-47D cells. Collectively the results show that epigenetic changes associated to acetylation of proteins in general affect the energy metabolism in all cancer cell lines and that mitochondria may occupy a central role in metastasis. J. Cell. Biochem. 116: 797–808, 2015.

KEY WORDS: BREAST CANCER; MITOCHONDRIAL PHYSIOLOGY; SODIUM BUTYRATE; TRICHOSTATIN A

Breast cancer, like all types of cancer, results from the subversion of multiple signaling pathways initiated by mutations in key regulatory genes, especially those that affect the cell cycle. The network that constitutes the control of the cell's homeostasis is so extensive and interlinked that when altered many cells undergo apoptosis. Those that survive occasionally respond by producing phenotypes that display the so called anti-social behavior summed up as the "hallmarks" of cancer [Hanahan and Weinberg, 2011].

Because of their central role in chromatin remodeling the histone acetylases (HATs) and histone deacetylases (HDACs) renamed as lysine acetyltransferases (KATs) and lysine deacetylases (KDACs) enzymes exert their effects not only on histones but on thousands of different proteins [Kim et al., 2006; Choudhary et al., 2009]. Many of these act in regulatory pathways and therefore, have been recognized as signal transmission nodes that reach processes well beyond the cell cycle [Choudhary et al., 2009]. At the level of histones, KDACs canonic mode of action involves the compaction of the complex DNA-protein and leads to repression of gene transcription. In breast cancer, for example, it is known that the some of the tumor suppressor genes whose products arrest the cell cycle are inactive as a consequence of the hyperactivity of

Conflict of interest: None.

Grant sponsor: CAPES; Grant sponsor: FAPERJ; Grant sponsor: FAF-ONCO; Grant sponsor: INCT/CNPq-Cancer; Grant number: 573806/2008-0.

*Correspondence to: Nivea Dias Amoêdo, Instituto de Bioquímica Médica Leopoldo De Meis, Universidade Federal do Rio de Janeiro, Av. Carlos Chagas Filho 373 BLE-22–Ilha do Fundão, Rio de Janeiro 21941-590, Brazil.
E-mail: amoedo@bioqmed.ufrj.br

Manuscript Received: 19 August 2014; Manuscript Accepted: 11 December 2014

Accepted manuscript online in Wiley Online Library (wileyonlinelibrary.com): 16 December 2014

DOI 10.1002/jcb.25036 • © 2014 Wiley Periodicals, Inc.

histone deacetylases. The use of histone deacetylases inhibitors (HDACis) such as trichostatin A (TSA) has been shown to favor the relaxation of the DNA-protein complex, thus allowing the activation of transcription of the relevant upstream and downstream regulatory cascade. In addition, as known today, the widespread acetylation and deacetylation of non-nuclear proteins can produce a myriad of effects by way of generating conformational alterations that influence their binding to different ligands. Hence, it has been possible to involve KATs and KDACs in multiple processes such as the modulation of chaperone proteins, the generation of free radicals and the regulation of inhibitors of the cell cycle [Buchwald et al., 2009].

Tumor cell metabolism is also differentiated. As a consequence of the peculiar energy requirements underlying the high rates of proliferation and migration and invasiveness in the case of metastatic cells, metabolic pathways that generate substrates that promote self-sufficiency have been selected [Amoedo et al., 2013]. Even though many pathways vary in cancer cells in general tumors could be roughly classified in two main groups in terms of ATP sources: those that are primarily glycolytic and those that preferentially carry out oxidative phosphorylation (OxPhos) [Moreno-Sanchez et al., 2014]. In both cases the fluxes of the pathways are dictated by a new order of regulation in which feedback mechanisms that normally inhibit rate-controlling steps are no longer fully operational. Such is the situation of isoforms of phosphofructokinase, for example, that are over expressed in tumor cells and which exhibit conformations that are less amenable to inhibition by ATP [Moreno-Sanchez et al., 2012; Coller, 2014].

An equivalent example in the Krebs cycle is that of the glutaminolysis derived α-ketoglutarate which literally reverses the vectorial sense of the cycle, thus producing citrate and acetyl-CoA and leading ultimately to fatty acid synthesis [Mullen et al., 2012]. Other links between altered cell metabolism and the activity of KATs have been established. The recent finding that in pancreatic cancer, lactate dehydrogenase is negatively regulated by lysine acetylation emphasizes the point [Zhao et al., 2013]. In this case, acetylation was found, among other effects, to mark the enzyme for degradation by autophagy. Many more pathways that include protein substrates for KATs and KDACs have been reported. For example, five major intermediary metabolism pathways (glycolysis, glycogen metabolism, fatty acid metabolism, the tricarboxylic acid cycle and the urea cycle) contain enzymes that are acetylated. Although the overall effects of acetylation/deacetylation on the activities of these enzymes has not been fully unraveled, some patterns are emerging that indicate that the fluxes and the directions of the pathways themselves can be regulated in this manner. For instance, it has been found that acetylated glyceraldehyde 3-phosphate dehydrogenase (GAPDH) favors glycolysis, whereas deacetylation of the enzyme increases gluconeogenesis [Guan and Xiong, 2011; Zhao et al., 2013; Li et al., 2014]. Thus, when glucose is freely available, glycolysis will take place. Alternatively, when acetate is present gluconeogenesis will prevail. In the TCA cycle, malate dehydrogenase activity is activated by acetylation in a reversible fashion, thus illustrating how the cycle itself can be modulated by the acetate adducts. Likewise for succinate dehydrogenase and isocitrate dehydrogenase 2, two enzymes that have key roles in determining which metabolites are going to be produced or consumed and whether the cells will find themselves in an anabolic or catabolic status. Conceivably, the regulation of other pacemaker switches by acetylation/deacetylation, particularly at the cytoplasm-mitochondrial interface can be regarded as having high relevance for cancer cells given the plasticity that it confers. Thus, it can be predicted that by dissecting the different biochemical subtypes present in tumor cells it may be possible to recognize how and when they acquire the ability to circumvent the barriers naturally imposed on normal cells. The broad range of activities of HDACs suggests that HDACis would be useful as shotgun strategies for the treatment of cancer. By the same token one could predict a plethora of side effects of HDACis due to HDACs pleiotropic roles. Curiously, however, HDACis seem to act preferentially on tumor cells, a trait that is still not completely understood. We have thus chosen an experimental model consisting of cell lines of breast cancer bearing progressive malignant phenotypes and enquired about the effects of HDACis sodium butyrate and trichostatin A on the glycolytic and oxidative pathways of these cells. With this approach we hoped to find clues that could explain why tumor cells are more susceptible to HDACis.

MATERIALS AND METHODS

CELL CULTURE

The cells were kindly provided by Dr. Claudia Gallo (Roberto Alcântara Gomes Biology Institute, Rio de Janeiro State University, Brazil). MCF-10A, a human breast non-tumorigenic epithelial cell line, was maintained in DMEM-F12 medium supplemented with fetal bovine serum (FBS) 10%, EGF 0.02 μg/mL, insulin 5 μg/mL, and hydrocortisone 1.25 μg/mL, pH 7.4. MCF- 7, T47-D and MDA-MB-231, human breast cancer epithelial cell lines, were grown in RPMI-1640 medium supplemented with FBS 10%, pH 7.4. All the cell lines were maintained at 37°C in a humidified incubation chamber with CO_2 5% and the cells were sub-cultured every 2 days and used on experiments when they reached 85% confluence. All cell lines were genotyped and periodically checked for mycoplasma contamination.

CELL VIABILITY AND CYTOTOXICITY ASSAY

For those assays the cells were grown on 24 and 96 well plates. 24 h after plating, cells were incubated with different concentrations of NaB and for 24 or 48 h. After each treatment, cell viability was accessed using MTT and SRB assay, as described previously [Mosmann, 1983; Skehan et al., 1990]. The cytotoxicity was assayed by lactate dehydrogenase (LDH) release after NaB or TSA treatment using CytoTox96 Non-radioactive Cytotoxicity assay kit (Promega).

SOFT AGAR COLONY FORMATION ASSAY

3.10^4 cells control were cultured in the presence or absence of NaB in a 6-well plate containing RPMI supplemented with 10% FBS and solidified with agar. Fresh medium were added twice weekly. The plates were incubated for 21 days, and colonies with diameters greater than 50 μm were then scored as positive, using a phase-contrast microscope equipped with a measuring grid.

GLUCOSE UPTAKE

Cells were grown in six well plates and treated with NaB 2 mM for 24 h. After the treatment, the culture medium was replaced by fresh

medium without glucose supplemented with 100 μM of 2-NBDG for 30 min at 37°C in a humidified incubation chamber with CO_2 5%. The cells were pelleted (1,000 *x g* for 5 min at 4°C) and ressuspended in 300 μL of PBS 1X. Samples were analyzed in FACSCalibur flow cytometer (Becton Dickinson) using CellQuest software (Becton Dickinson), respectively, for data acquisition and analysis.

KINETICS OF LACTATE RELEASE IN THE CULTURE MEDIA

After the treatment with different concentrations of NaB and TSA for 24 h, the culture media were replaced by fresh RPMI 1640 medium without phenol red and FBS. At the indicated times (0, 15, 30, 40, 50, and 60 min), aliquots from culture medium were collected and lactate measurement was performed in a hydrazine/glycine buffer (pH 9.2), containing β-NAD^+ 5 mg/mL and lactate dehydrogenase 15 units/mL. The absorbance due to formation of NADH was monitored in a microplate reader (SpectraMax M5, Molecular Devices) at 340 nm and was correlated with the presence of lactate on samples from a standard curve [Hamilton and Pardue, 1984].

PREPARATION OF MITOCHONDRIAL AND CYTOSOLIC PROTEIN FRACTIONS

The cell pellets were mixed to a lysis buffer contained Tris-HCl 10 mM pH 7.4, sucrose 0.25 M, NaF 20 mM, DTT 1 mM, EDTA 5 mM, PMSF 1 mM, and protease inhibitors cocktail (quimostatin, leupetin, antipain, pepstatin A – Sigma-Aldrich). The cell suspension was transferred to homogenizers (Wheaton Potter-Elvehjem) for cell lysis. The suspension was centrifuged at 100 *x g* for 5 min at 4°C, the pellet with debris was discarded and the resulting supernatant was centrifuged at 10,000 *x g* for 15 min at 4°C. Then the supernatant (cytosolic fraction) was used for measurement of the recovered activities of HK, PYK, LDH, and G6PDH and the pellet (mitochondrial enriched fraction) was used for measurement of the recovered activities of mt-HK and CS. Protein concentration was performed using the Bradford method.

ENZYMATIC ACTIVITY ASSAYS

Enzymatic activities were measured using the following reaction media: (a) for HK, Tris-HCl 20 mM pH 7.4, $MgCl_2$ 10 mM, β-NAD^+ 1 mM, G6PDH (*Leuconostoc mesenteroides*) 1 unit/mL, Triton X-100 0.1%, ATP 2 mM, and glucose 5 mM. (b) For PYK, Tris-HCl 50 mM pH 7.4, $MgCl_2$ 5 mM, KCl 50 mM, β-NADH 0.2 mM, ADP 2.5 mM, Triton X-100 0.1%, phosphoenolpyruvate 5 mM, lactate dehydrogenase 0.5 units/mL. (c) For LDH, Tris-HCl 50 mM pH 7.4, EDTA 1 mM, β-NADH 0.2 mM, Triton X-100 0.1%, pyruvate 1 mM. (d) For G6PDH, Tris-HCl 50 mM pH 7.4, $MgCl_2$ 5 mM, Triton X-100 0.1%, glucose-6-phosphate 2 mM and β-NADH 0.2 mM. The reaction started with the addition of 5–140 μg protein and was carried out at 37°C for 5–10 min. After incubation, the samples were immediately boiled and placed in ice. Absorbance was measured at 340 nm and the value used to calculate the specific activity of the enzymes was defined as the amount of substrate formed per milligram of protein per minute. For CS, Tris-HCl 50 mM pH 8.1, acetyl-CoA 0.3 mM, Triton X-100 0.1%, DTNB 0.1 mM, oxaloacetate 0.5 mM. The reaction was started by the addition of 10 μg protein and carried out at 30°C for 5 min. Absorbance was measured at 412 nm.

OXYGEN CONSUMPTION OF INTACT CELLS

O_2 consumption rates were measured polarographically using high-resolution respirometry (Oroboros Oxygraph-O2K). After the treatment period, medium was removed and cells were either suspended in RPMI for measurements of O_2 consumption of intact cells. Routine consumption, oligomycin-independent respiration (proton leak) and FCCP-stimulated respiration (maximum respiration) were measured in intact cells as described previously [Hutter et al., 2004]. DatLab software (Oroboros Instruments, Innsbruck, Austria) was used for data acquisition and analysis.

RNA EXTRACTION AND cDNA SYNTHESIS

Total RNA was isolated from cells using TRIzol reagent (Invitrogen) according to the manufacturer's instructions. Total RNA was quantified spectrophotometrically and 1 μg were treated with 1 U of DNAse RNAse-free for 30 min at 37°C. Reactions were stopped by adding 1 μL of EDTA 20 mM and heating for 10 min at 65°C. cDNA synthesis was performed using the DNAse treated RNA according to High Capacity cDNA Reverse Transcription Kit from Applied Biosystems.

REAL TIME PCR

The gene expression analysis was performed using a 7500 Real Time PCR (Applied Biosystems) and power SYBR-GREEN PCR master MIX (Applied Biosystems). For this test primer pairs were synthesized based on GenBank mRNA sequences. The sequences of the primers are presented in supplementary methods (Table S1). The comparative Ct method was used to compare changes in gene expression levels [Livak and Schmittgen, 2001]. Actin expression was used as an endogenous control.

STATISTICAL ANALYSIS

Statistical analysis was performed using Graph Pad Prism 6. The results are expressed as means ± S.E.M for *n* independent experiments. Statistical significance was determined by Student's *t*-test and one-way ANOVA.

RESULTS

BASIC METABOLIC PROFILE IN BREAST CANCER CELL LINES: MDA-MB-231 HAS A HIGHER LACTATE RELEASE AND GLUCOSE UPTAKE AND MCF-10A AND MCF-7 HAVE A HIGHER RESPIRATORY CAPACITY

Prior to the experiments measuring the effects of sodium butyrate and tricostatin A, the cell lines MCF-10A, MCF-7, T-47D and MDA-MB-231 were evaluated for a series of biochemical parameters that included lactate release, glucose uptake and oxygen consumption. The results in Figure 1A–C, show that the highly metastatic MDA-MB-231 cells has a higher lactate release and glucose uptake compared to the other lines. MCF-7 and T-47D cells occupied an intermediary position. Addition of antimycin A (AA) to the incubation medium changed somewhat the lactate release profiles (Fig. 1C). T-47D cells were insensitive to AA, whereas the inhibitor induced in MDA-MB-231 and MCF-7 the highest rates of lactate release followed by MCF-10A. By way of explaining these results it

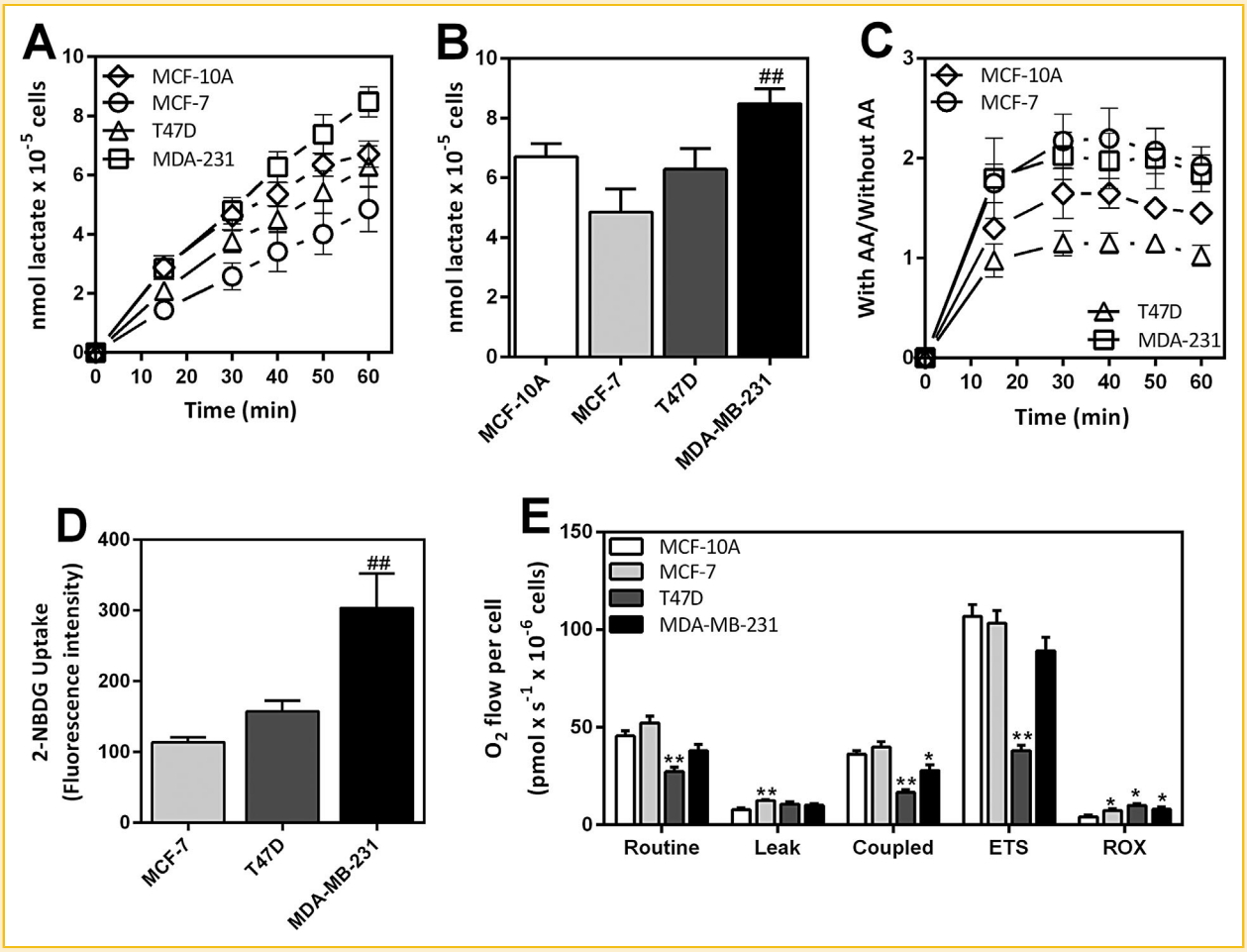

Fig. 1. Basic metabolic profile in breast cancer cell lines: MDA-MB-231 has a higher lactate release and glucose uptake and MCF-10A and MCF-7 have a higher respiratory capacity. (A) Kinetics of lactate release of MCF-10A, MCF-7, T47D, and MDA-MB-231. (B) Lactate release after 60 min. (C) 2 μg/mL antimycin A was added to the culture. Aliquots of the supernatant were taken at 10 min intervals and lactate released was measured. Lactate production ratio of breast cancer cells in the presence or absence of antimycin A shows the stimulation of lactate production upon inhibition of oxidative phosphorilation. (D) Glucose uptake. Values represent mean ± SEM; N = 4; $^{\#\#}P < 0.01$, compared with MCF-7 line. (E) Respiration of intact MCF-10A, MCF-7, T47D, and MDA-MB-231 cells was measured under routine conditions (ROUTINE), inhibition by oligomycin (LEAK), uncoupling to maximum flux (ETS) and inhibition by rotenone and antimycin A (ROX). The routine, leak and ETS parameters were corrected by ROX subtraction. Values represent mean ± SEM; N = 10. $^{*}P < 0.05$; $^{**}P < 0.01$, compared with MCF-10A.

may be relevant to comment that the cell lines used in the present work do vary in their OXPHOS complex protein levels. Reports on mitochondrial biogenesis and dynamics induced by 17β-estradiol have shown a differential response to the steroid that was related to intrinsic OXPHOS properties of these cells [Sastre-Serra et al., 2013]. Furthermore, the activities and gene expression levels of complex I-V have been assayed revealing dramatic differences, especially of complex III, between normal and aggressive metastatic breast cancer cells [Owens et al., 2011]. In short, it is plausible to invoke individual differences in the components of the electron transport system or even in the conformation of the super complexes that would afford the tumor cells with peculiar properties involving respiration, particularly by considering that the cell lines used here do in fact have different ontogenies.

The cell lines also differed in their ability to incorporate glucose. Figure 1D, show that MDA-MB-231 cells displayed the highest rates of glucose uptake, a result which was consistent with the higher expression of glucose transporter GLUT 1 by the same cell line, as depicted in Figure S1-A, MDA-MB-231 cells showed a higher expression of LDH (Fig. S1-B) relative to MCF-7 and T-47D. Results using high resolution respirometry show that oxygen consumption in MCF-10A, MCF-7, and MDA-MB-231 exhibited similar values in all the respiratory parameters analyzed and that T-47D cells had the lowest values as shown (Fig. 1E). This result also show that the MDA-MB-231 cells are not strictly glycolytic, since they displayed an OXPHOS capacity similar to MCF-10A, a non-tumorigenic cell line.

T47-D CELLS ARE MORE SENSITIVE TO SODIUM BUTYRATE AND TRICOSTATIN A THAN THE OTHER BREAST CANCER CELLS

In order to evaluate the true effects of sodium butyrate and tricostatin A on the metabolic parameters of the cell lines, care was taken to carry out the experiments within an adequate concentration range of the

inhibitors, that is, concentrations that would not mask general HDACi-related cytotoxic effects. Cells were analyzed for viability and proliferation using the MTT and SRB assay after incubation with NaB (2–10 mM) and TSA (0.01–1 μM). The cells responded in a time and dose dependent manner. In Figure 2A, it can be seen that only T-47D cells were affected by incubation with 2 mM NaB for 24 h as compared to MCF-10A, MCF-7, and MDA-MB-231. This pattern was maintained after 48 h incubation with 2 mM NaB as shown in Figure 2B. Consistently, the results in Figure 2D–E show that 2 mM NaB reduced the growth of T-47D cells, although after 48 h, only MCF-10A cells

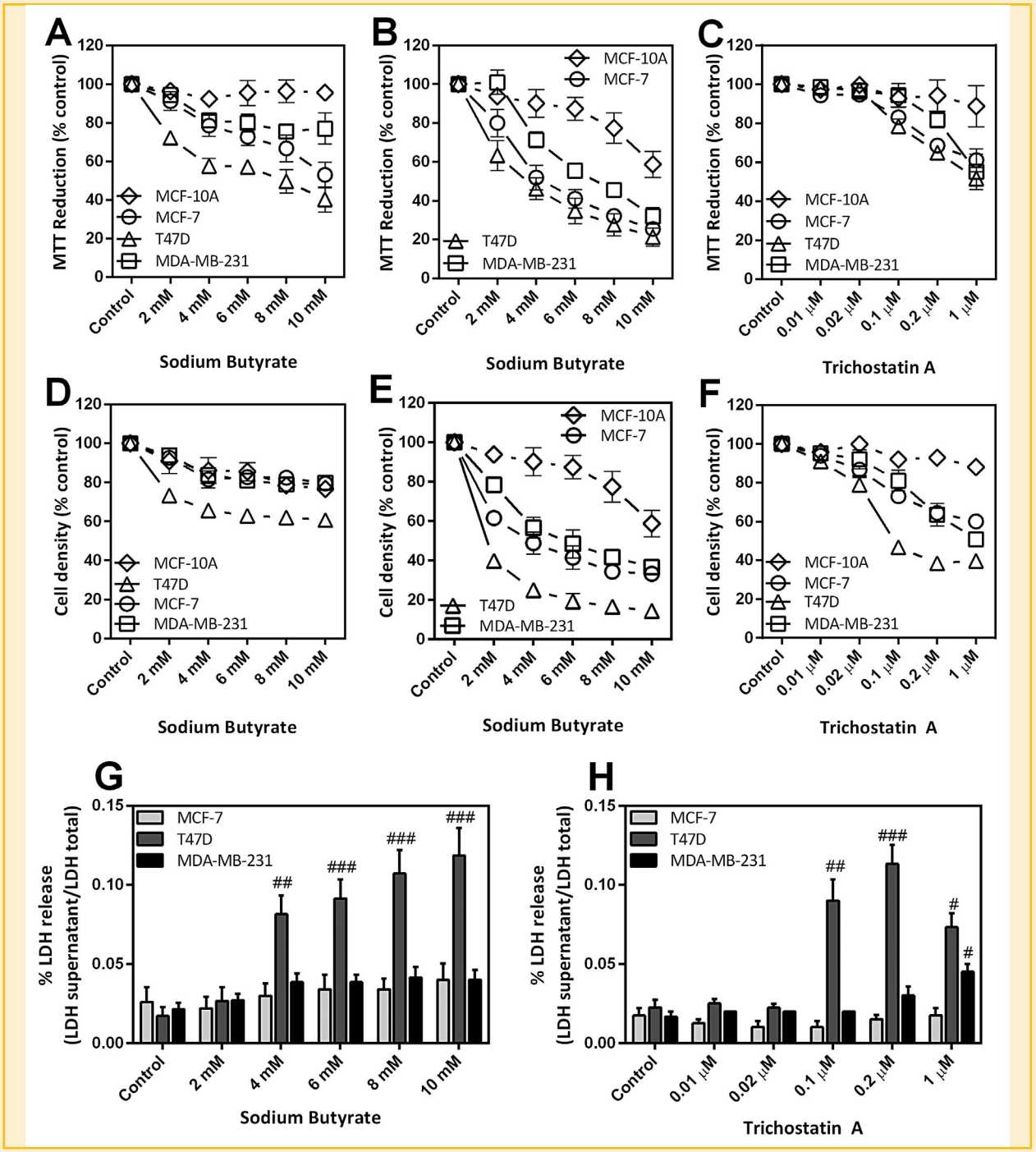

Fig. 2. Sodium butyrate (NaB) and trichostatin A (TSA) induce time and dose-dependent growth down-regulation in breast cancer cells. Cells were incubated in the presence of various concentrations of NaB or TSA 24 or 48 h. At indicated times, viability was analyzed by MTT assay for 24 (A, C) and 48 h (B), respectively. Proliferation was analyzed by SRB assay for 24 (D, F) and 48 h (E), respectively. Also, citotoxicity (G, H) was estimated by measurement of lactate dehydrogenase (LDH) release after NaB or TSA treatment using CytoTox96 Non-Radioactive Cytotoxicity Assay Kit (Promega). Values represent mean ± SEM; N = 5; $^{\#}P < 0.05$; $^{\#\#}P < 0.01$; $^{\#\#\#}P < 0.001$, compared with control.

seemed to be unaffected by 2 mM NaB. Essentially, the same results were obtained when these experiments were repeated with TSA, using concentrations spanning 0.02–1 μM (Fig. 2C, E, and F). When the cell lines were compared for NaB induced cytotoxicity by measuring LDH release. The results in Figure 2G show that only T-47D cells released LDH and even so at 4 mM NaB. Figure 2H, show the results of cell viability, growth and LDH release in the presence of TSA. Cell viability, inhibition of cell growth and LDH release were only clearly apparent at 100 nM concentration. Therefore, unless otherwise stated for the remaining experiments the cells were incubated during 24 h with 2 mM and 20 nM NaB and TSA, respectively. To confirm the hypothesis that treatment with NaB and TSA for 24 h was cytostatic and not cytotoxic to the cells were subjected to a detailed analysis of the cell cycle profile by flow cytometry (Fig. S2) precaution ensured that the results obtained here reflected the cellular response to prime HDACis targets, rather than a widespread cytotoxicity with the implied repression of metabolic parameters generated by high TSA dosage as observed elsewhere [Sun et al., 2014]. It is important to note non-tumorigenic MCF-10A cells were less sensitive to NaB and TSA with regards to proliferation and cycle arrest. Thus, this cell line could be an important model to investigate the cellular resistance by exposure to different HDACis.

The selectivity displayed by the treatment of cells with the HDACis shown in Figure 2 was not paralleled by experiments in which NaB was incubated with the cell lines in 3D culture systems. The results in Figure 3 show that colony formation was equally and dramatically inhibited by 2 mM NaB in all experimental groups. Because in 3D cultures the spatial organization of cells reflect more realistically the tumor situation, the results in Figure 3 suggests that lower doses of the inhibitor may be sufficient for in vivo experiments.

SODIUM BUTYRATE (NAB) REDUCES THE GLYCOLYTIC PATHWAYS IN MCF-7 AND T47-D CELLS, BUT HAD NO EFFECT ON LACTATE RELEASE OF MCF-10A AND MDA-MB-231

Sodium butyrate 2 mM was able to reduce lactate release by MCF-7 and T-47D cells in contrast to MCF-10A and MDA-MB-231 which were unaffected as shown in Figure 4. This effect could not be correlated to glucose uptake because NaB did not influence that parameter in MCF-7 and T47-D cells. Furthermore, there were no alterations in GLUT 1 expression (Fig. S3). Regarding the other glycolytic flux regulators, T-47D cells were the only ones in which NaB stimulated HK1 expression significantly. In contrast, except for MDA-MB-231 cells, HK2 expression was inhibited by NaB in the other cells. This profile was reproduced when hexokinase activity was assayed as shown in Table I. The results suggest that in T-47D cells mitochondria bound HK was preferentially affected by the inhibitor.

Experiments measuring the effect of NaB on the expression of LDH-A and LDH-B and on the monocarboxylate transporters MCT1 and MCT4 were carried out next. The results in Figure 5A–D show again that T-47D cells were the only cell line that responded in a differentiated manner to NaB. Given the kinetics of the LDH-B isoform favoring the formation of pyruvate from lactate, the dramatic increase in the expression of LDH-B as a result of NaB action may explain the results described in Figure 4C in which the inhibitor decreased lactate release. That pyruvate was not being preferentially synthesized from phosphoenolpyruvate through pyruvate kinase activity was shown by experiments in which the activity of the enzyme did not seem to suffer any stimulatory effect by NaB Table I. This interpretation, however, does not hold for the MCF-7 cells in which LDH-B expression was not affected by NaB (Fig. 5B). LDH activity was found to be increased after NaB treatment only in T-47D cells (Table I), once more evidencing the sensitivity of those cells to the inhibitor and this result suggests that NaB induces an increase in the oxidation of lactate in these cell line once an increase in expression in LDH-B was observed.

Monocarboxylate transporter (MCT1) expression was also increased in T-47D cells, followed by MDA-MB- 231, when they were incubated in the presence of NaB (Fig. 5C and D). Ultimately, the action of NaB depends on its intracellular concentration. The fact that NaB is also transported by MCT1 [Goncalves and Martel, 2013], must create a loop in which NaB progressively accumulates within the cells and as a

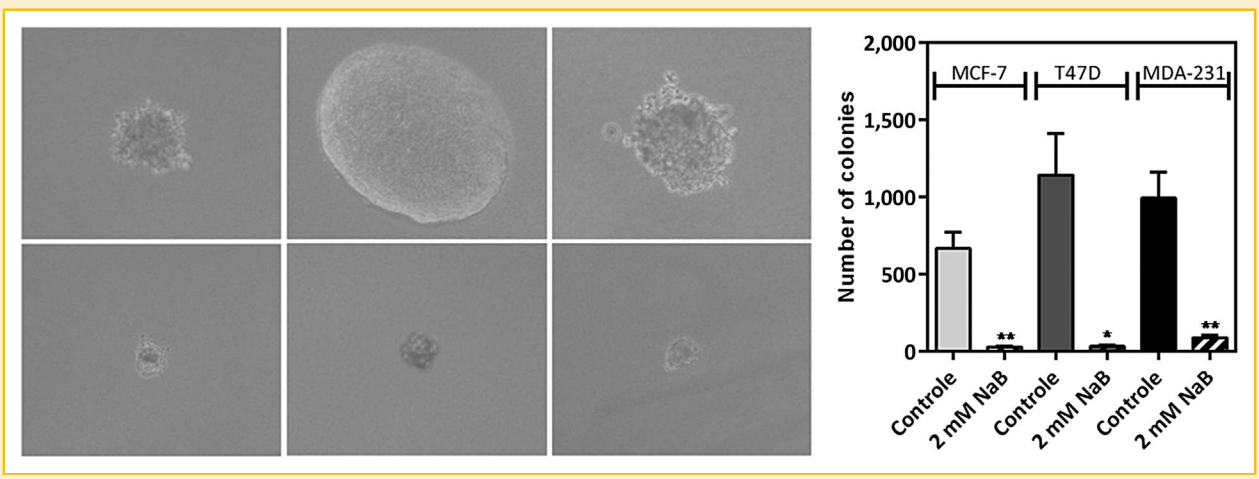

Fig. 3. The anchorage-independent growth of MCF-7, T-47D, and MDA-MB-231 cells was equally and dramatically inhibited by 2 mM NaB. Representative cell colonies in soft agar are shown. Quantitative analysis of colony numbers is shown in the right side. Values represent means ± SEM; N = 3. $^{*}P < 0.05$; $^{**}P < 0.01$, compared with control.

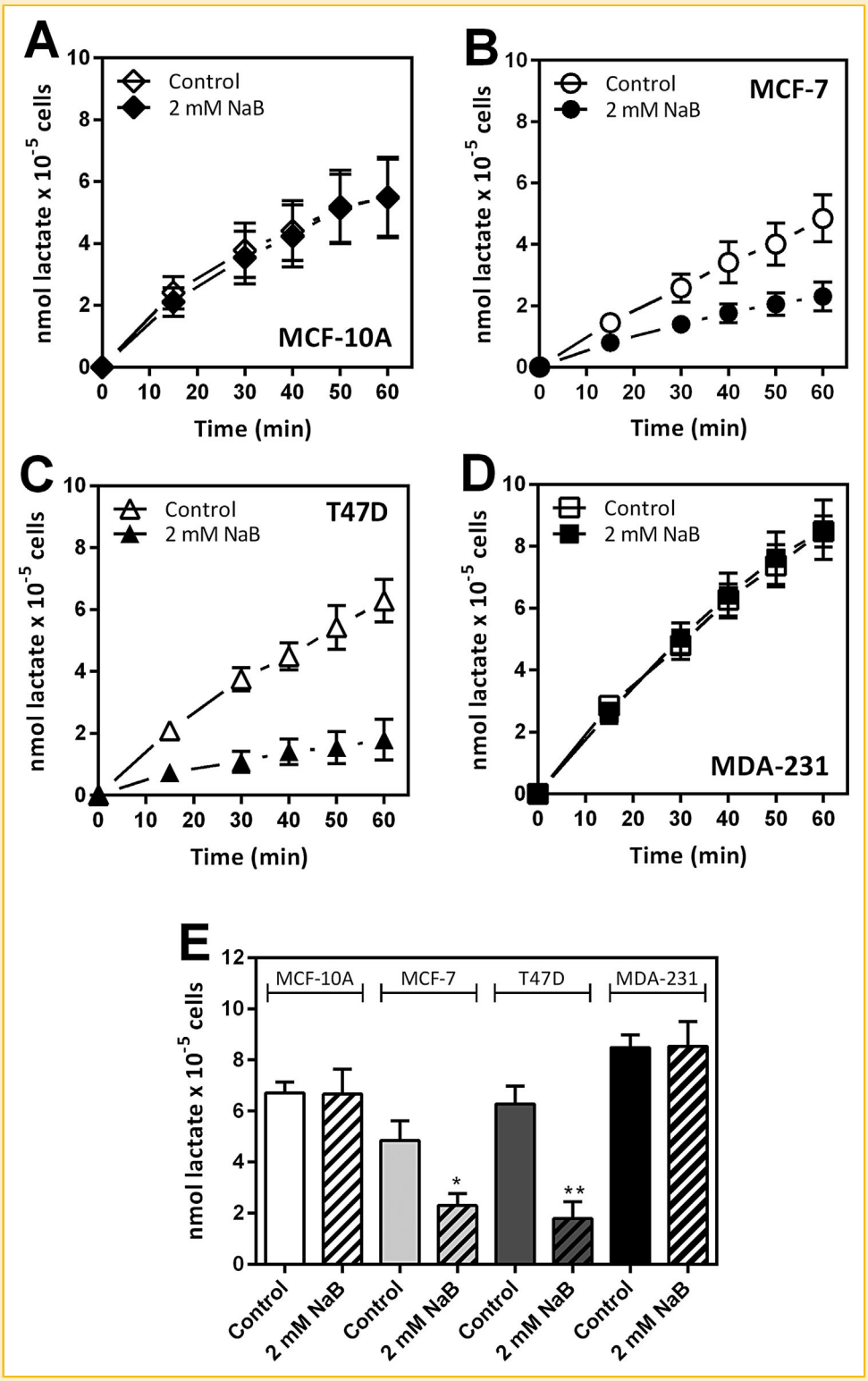

Fig. 4. Sodium butyrate (NaB) reduces glycolytic pathways in MCF-7 and T47D cells. However, NaB has no effect on lactate release in MCF-10A and MDA-MB-231. Kinetics of lactate release of (A) MCF-10A, (B) MCF- 7, (C) T47-D, and (D) MDA-MB-231. (E) Lactate release after 60 min. Values represent mean ± SEM; N = 4. $^{*}P < 0.05$; $^{**}P < 0.01$, compared with control.

TABLE I. Effect of Sodium Butyrate on Hexokinase (HK), Pyruvate Kinase (PYK) and Lactate Dehydrogenase (LDH) Activities from Breast Cells

	Specific Activity (μmol NADH $\times$ mg^{-1} $\times$ min^{-1})					
	MCF-7		T47-D		MDA-MB-231	
	Control	NaB	Control	NaB	Control	NaB
HK[(a)]	0.03 ($\pm$0.007)	0.03 ($\pm$0.002)	0.04 ($\pm$0.008)	0.04 ($\pm$0.006)	0.05 ($\pm$0.005)	0.041 ($\pm$0.009)
mit-HK[(b)]	0.10 ($\pm$0.01)	0.10 ($\pm$0.02)	0.14 ($\pm$0.02)	0.09 ($\pm$0.03)	0.11 ($\pm$0.007)	0.095 ($\pm$0.014)
PYK[(c)]	6.3 ($\pm$0.7)	7.7 ($\pm$0.6)	7.8 ($\pm$0.4)	8.6 ($\pm$0.5)	7.6 ($\pm$0.5)	9.3* ($\pm$0.3)
LDH[(d)]	2.5 ($\pm$0.2)	3.1 ($\pm$0.5)	3.9 ($\pm$0.4)	5.8* ($\pm$0.5)	7.2 ($\pm$0.6)	7.9 ($\pm$0.5)

Specific HK activity present in cytosolic (a) and mitochondrial (b) fraction, respectively, of was assayed using an enzymatic assay coupled to glucose 6-phosphate dehydrogenase. Values represent mean $\pm$ SEM; N = 5. Specific PYK (c) activity assayed by an enzymatic assay coupled to lactate dehydrogenase. (d) Specific LDH activity present in cytosolic fraction of breast cancer cells. Values represent mean $\pm$ SEM; N = 5.
*$P < 0.05$, compared with control.

consequence facilitates the transport of other monocarboxylates. The results shown in Figure 4, particularly in T47-D, cells could be interpreted as resulting from both: a higher influx of NaB which in turn promoted the super-expression of MCT1 and the entry of lactate into the cells (MCT1 is known to displace monocarboxylate transport inwards rather than outwards). It must also be mentioned that NaB cannot itself be considered a metabolite since control experiments showed that NaB does not increase oxygen consumption when added to respiring cells (data not shown). In the other cell lines, expression of MCT1 and MCT4 was not as significant (Fig. 5).

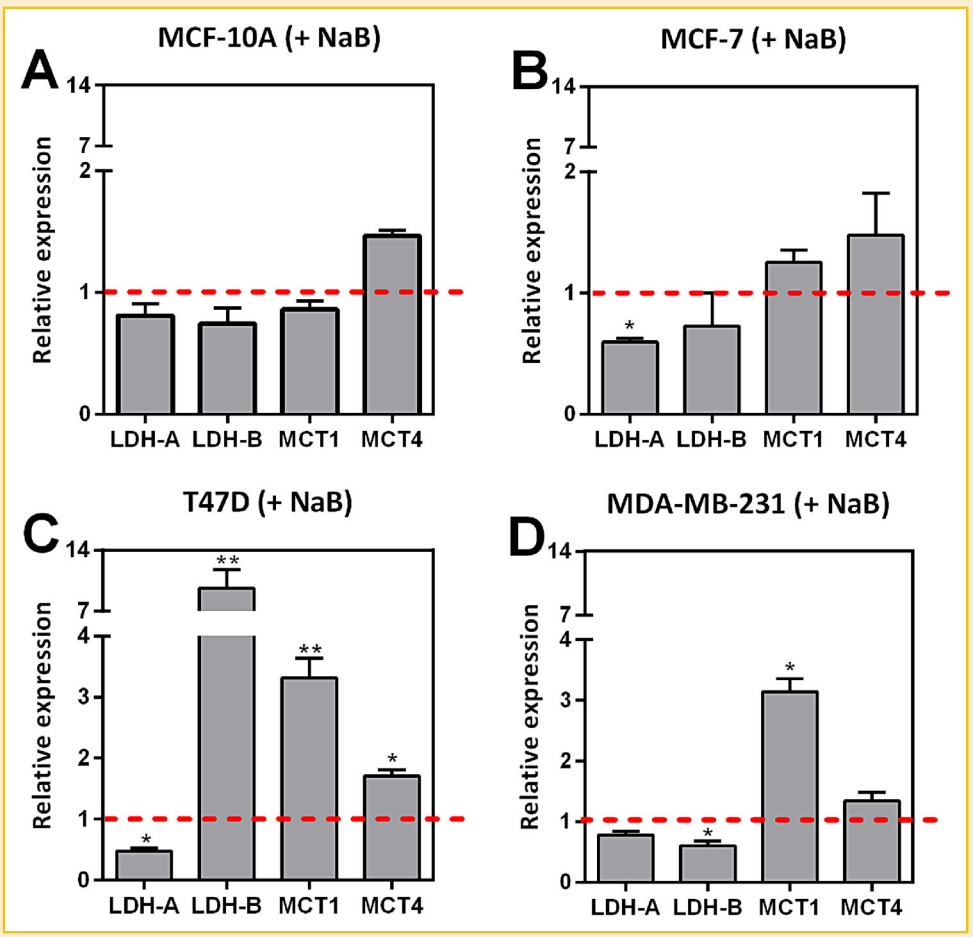

Fig. 5. Sodium butyrate (NaB) treatment regulates LDH-B and MCT 1 transcription. Cells were treated with NaB 2 mM for 24 h and LDH-A, LDH-B, MCT1, and MCT-4 expressions were determined by Real Time PCR. (A) MCF-10A, (B) MCF-7, (C) T47-D, and (D) MDA-MB-231. Actin was used to normalize cDNA amounts. The dashed line represents the control. Values represent mean $\pm$ SEM; N = 3, *$P < 0.05$; **$P < 0.01$, compared with control.

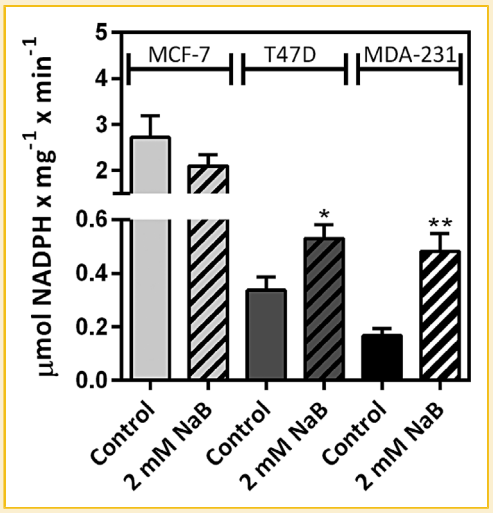

Fig. 6. Treatment with sodium butyrate (NaB) increase G6PDH activity in T47-D and MDA-MD231 cells. Specific glucose-6-phosphate dehydrogenase activity in cytoplasmic fraction of breast cancer cells. Values represent mean ± SEM; N = 5; $^{*}P < 0.05$; $^{**}P < 0.01$, compared with control.

NAB INCREASES G6PDH ACTIVITY IN T47-D AND MDA-MD231 CELLS. AN ANTI-OXIDANT RESPONSE?

The NaB induced glucose uptake observed for MDA-MB-231 cells (Fig. S3-E) without any significant increase in either the expression or activity of hexokinase (Fig. S3-D and Table I) prompted us to investigate whether other pathways utilizing the sugar could be involved. Therefore, we carried out experiments to determine whether the activity of the rate-limiting enzyme of the pentose phosphate pathway (PPP), glucose-6-phosphate dehydrogenase (G6PDH) was altered in the presence of NaB. The results in Figure 6 show that in T-47D and MDA-MB-231 cells the activity of G6PDH was stimulated by NaB, particularly the latter in which approximately a 3 fold increase in activity was observed. In MCF-7 cells G6PDH activity was slightly reduced. The results suggest that in T-47D and MDA-MB-231 cells the enhanced NaB mediated increase in G6PDH activity may represent a switch triggered either by direct acetylation of the enzyme or of an alternative pathway. This would be compatible with more aggressive phenotypes in which the high rates of proliferation would require the availability of NADPH and of pentoses for nucleic acid and coenzyme synthesis. However, direct acetylation of glucose 6-phosphate dehydrogenase was shown to

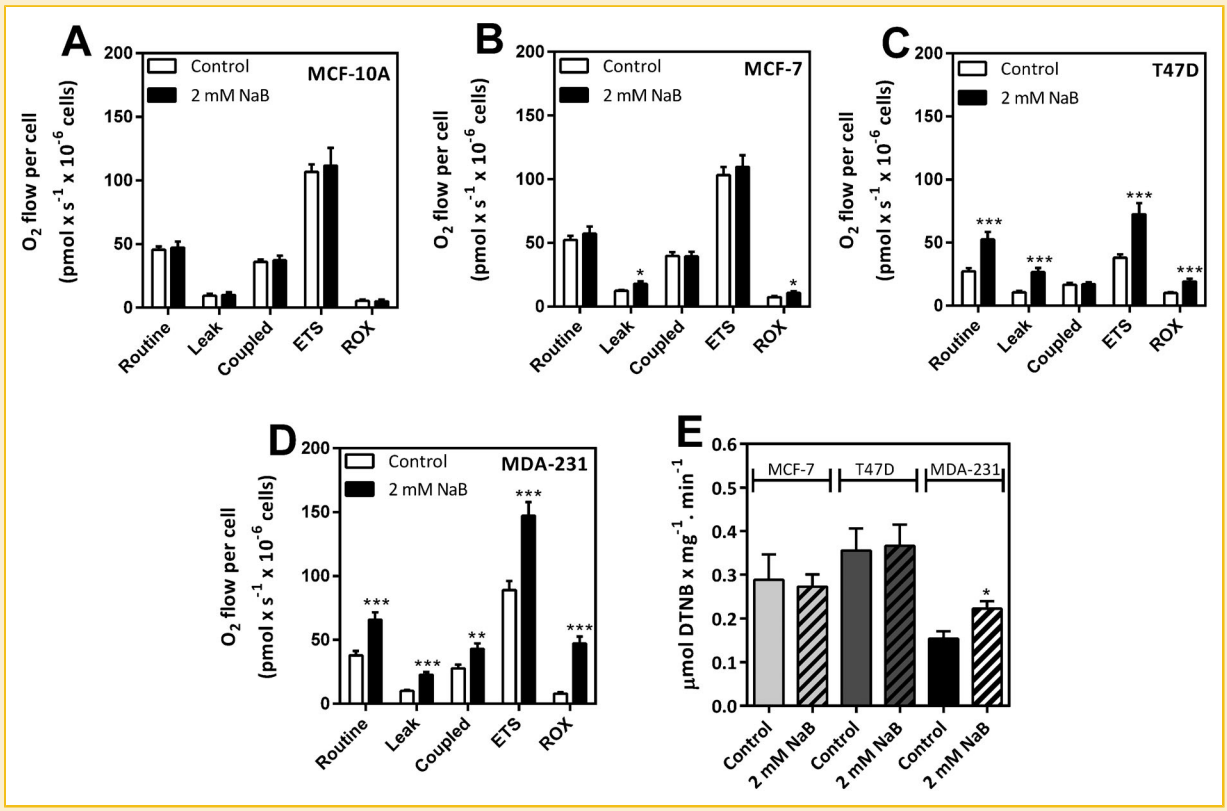

Fig. 7. Treatment with sodium butyrate (NaB) induces different effects on mitochondrial respiratory parameters in intact breast cancer cells. Mitochondrial respiratory parameters were performed in high- resolution oxygraph (O2k, Oroboros Inc.). After treatment with 2 mM NaB for 24 h, MCF-10A, MCF-7, T47D, and MDA-MB-231 cells oxygen flow was measured on RPMI medium (with glucose, without fetal bovine serum). Respiratory parameters of (A) MCF-10A, (B) MCF-7, (C) T47-D, and (D) MDA-MB-231 cells. Respiration of intact cells was measured under routine conditions (ROUTINE), inhibition by oligomycin (LEAK), uncoupling to maximum flux (ETS) and inhibition by rotenone and antimycin A (ROX). The routine, leak and ETS parameters were corrected by ROX subtraction. Values represent mean ± SEM; N = 10; $^{*}P < 0.05$; $^{**}P < 0.01$; $^{***}P < 0.001$, compared with control. Sodium butyrate treatment increases the mitochondria content in MDA-MB- 231 cells. (E) Specific citrate synthase activity present in mitochondrial fractions of breast cancer cells treated with 2 mM NaB for 24 h. Values represent mean ± SEM; n = 5. $^{*}P < 0.05$ compared with control.

produce the opposite effect [Wang et al., 2014]. Presumably, in MDA-MB- 231 and to lesser extent in T-47D cells, the observed NaB effect on G6PDH corresponds to an anti-oxidant response unrelated to the PPP. Indeed, results linking NaB and TSA treatment of the same cell lines used in this work with superoxide dismutase expression have shown that MDA-MB-231 and T-47D clearly responded to NaB treatment by increasing the levels of SOD2, whereas in MCF-7 the HDACis inhibited transcription [Hitchler et al., 2008]. The authors proposed that the observed effect of the HDACis was associated to the overall chromatin structure which reacts to the acetylation/deacetylation balance by becoming more or less accessible to diverse ligands. However, the precise mechanism of the NaB mediated activation of anti-oxidant reactions involved in the maintenance of the redox equilibrium still remains to be clarified. Within that context it must be kept in mind that other scavenging systems besides SOD2 may also be responsive to the HDACis.

TREATMENT WITH SODIUM BUTYRATE (NAB) INDUCES AN INCREASE ON MITOCHONDRIAL RESPIRATORY PARAMETERS IN T47 -D AND MDA-MD231 CELLS

The results presented in Figure 7A–D are consistent with the idea that the tumor cell lines investigated respond in an individual manner to NaB. The patterns obtained show that only in T-47D and MDA-MB-231 cells, NaB was able to promote an enhancement of oxygen consumption when all respiratory parameters were measured. This result can be associated with an increase in mitochondrial content induced by NaB in MDA-MD231 cells (Fig. 7E). The same effect was not observed in others cells. The observation that the effects described above did require a long term pre-incubation with NaB is noteworthy. Control experiments in which NaB was added to the cells directly into the oxygraph during 30 min prior to the actual measurements of oxygen consumption showed that the inhibitor produced no significant differences when the cell lines were compared (Fig. S5). Besides indicating NaB is in fact acting at the level of protein deacetylases, the results also show that concentrations of NaB of 0.5 and 2 mM are in no way harmful to the cells as judged by a parameter, namely oxygen consumption that reflects the overall health of the cells. Interestingly, in Figure 7 we observed an increase in oxygen consumption in presence of rotenone and AA (ROX) in all tumorigenic lines, according to the degree of tumorigenicity, suggesting that NaB can induce the activity of other oxygenases once rotenone and AA are compounds that canonically abolish mitochondrial function. Conceivably in these cells oxidases external to the mitochondria are operative and upon treatment with the HDACis contribute significantly to oxygen consumption. Candidates are NADPH oxidases of the endoplasmic reticulum. Interestingly, when MDA-MB-231 cells treated with rotenone and AA were incubated in the presence of NaB and TSA and increasing concentrations of the non-specific NADPH oxidase inhibitor diphenyliodonium (DPI), there was a significant drop in the oxygen consumption comparable to the levels remaining after rotenone and antimycin A poisoning. The results are shown in Figure S4. These results raise the questions of why only MDA-MB-231 cells would have functional NADPH oxidases and whether those are up regulated by acetylation.

DISCUSSION

Since the discovery that other non-histone proteins, involved in important cellular functions, can also be targets of acetylases and deacetylases there is a growing interest in the regulatory mechanisms associated to acetylation and deacetylation. Thus, in addition to chromatin remodeling and activation and repression of transcriptional process, the balance between acetylation and deacetylation has been shown to be critical to the normal functioning of various intracellular processes, including the regulation of energy metabolism. Naturally, these observations were extended to the alterations of the cellular biochemistry that are conducive to tumorigenesis. Indeed, recent studies have uncovered novel mechanisms and contexts in which different HDACs play critical roles in metabolic control. Taking that into consideration it is not surprising that HDACis as therapeutic drugs are experiencing a revival. For example, HDACis are currently being used in in combination with other drugs for the treatment of lymphoma [Grant et al., 2010; Falchook et al., 2013; Kaufman et al., 2013]. As mentioned above HDACis have the desirable feature of preferentially exerting their effects on tumor cells. The results obtained by us treating MCF-10 cell line with TSA and NaB have confirmed this peculiarity. We found that proliferation, modulation of glycolysis and oxidative phosphorylation were unaffected by the HDACis used here. Furthermore the inhibitors did not significantly alter the expression of several genes related to metabolism (Figure 4). At this stage the mode of action of TSA and NaB is not known and besides, cannot be generalized since individual types of tumors respond differently to these compounds [Chueh et al., 2014]. Hence, the answer as to why they are relatively nontoxic to normal cells must certainly lie on intrinsic properties of the cells themselves. For instance, it is known that epigenetic enzymes such as HDACs are often mutated in human tumors a situation that leads to their over expression in these cells. By assuming that the tumor cells are highly dependent on the HDACs, the HDACi induced hyper acetylation might be less tolerated by them because even a small reduction in the HDAC activity could abrogate the prevailing anti-apoptotic status established by over expression of the enzymes. Other factors could be important for the selectivity shown by the drugs such as their access to the targets. NaB is known to be transported by the proton-coupled monocarboxylate transporters MCT1 and MCT4 [Goncalves and Martel, 2013]. The results measuring the expression of the transporters showed that MCT1 is only over expressed by T47 D and MDA-MB-231 cells, indicating that these lines would indeed be more sensitive to the HDACis. In contrast, with the exception of MBA-MB-231, all the other cell lines over expressed MCT4, a transporter isoform which has a K_m 5–10 fold higher than MCT1. Presumably the net rates of transport of the HDACis of normal and tumor cells which may involve different influx- efflux kinetics also contribute to the differential sensitivity to the inhibitors. Nevertheless we cannot discard that major phenotypic differences between the cell lines occur that would involve the acetylation of transcription factors or of proteins members of several other signaling and metabolic pathways rather than just histones. For example, differential regulation mediated by acetylation affecting the activity ATP

citrate lyase (ACL), an important enzyme for the generation of acetyl-CoA (substrate for acetylation), is known to occur. [Wellen et al., 2009; Zaidi et al., 2012].

In addition, it is known that HDACis are capable of inducing the accumulation of ROS and thus promote cell death as a result of oxidative stress. Although the data in the literature does not throw any light on the selective effects of HDACis it is reasonable to assume that MCF-10 cells may have a more robust antioxidant system capable of protecting them from oxidative stress induced by the inhibitors [Ungerstedt et al., 2005; Xu et al., 2007; Lee et al., 2012]. In this context normal cells and tumor cells display distinct bioenergetic characteristics. Recent studies have uncovered novel mechanisms showing that HDACs play critical roles in how cancer cells obtain energy to survive. In the present work the results showed that cells in different stages of tumorigenic progression reacted differently to NaB which highlights the fact that they exhibit different metabolic profiles, especially in what concerns their energy status. Taken together, these results demonstrate that cell's bioenergetic profile has an impact on the effect mediated by HDACi and show the importance of tumor metabolic profiling before drug treatments. The results presented here suggest that in the more aggressive cell lines, the accessory energy afforded by the oxidative machinery that allows for migration and invasion may be accompanied by the ROS-related oxidative stress which in this situation must be countered by anti-oxidant systems by way of reactions not yet understood. The results also indicate that drug interference based on the combination of HDACis and inhibitors of the redox system may be a worthwhile strategy for treatment.

It is noteworthy that the changes observed in this set of breast cancer cells did not parallel the gradient of aggressiveness in terms of the metastatic behavior. The initial difficulty in interpreting the results reported here was to find functional coherence between the results involving the effect of the HDACis sodium butyrate and TSA on experimental models consisting of cell lines traditionally used in in vitro cancer research. In spite of the well-defined individual metastatic traits of the cell lines, one must not forget that they lack a unifying phenotype that would make the biochemical comparison a great deal more pertinent. In fact MCF-7 and T47D cells have been classified as ductal Luminal A and are low endocrine responsive. Furthermore MDA-MB-231 cells are grouped in the claudin-low slot, a criterion that relates its metastatic behavior to low expression of integral membrane proteins that make up tight junctions between adjacent cells [Holliday and Speirs, 2011]. Whilst this is a useful feature in terms of those aspects pertaining to migration and invasion of metastatic cells it is somewhat loose considering that the cells investigated here have significantly different gene expression signatures. Besides stressing these differences, collectively the results presented here hint at the possibility that the process of metastasis requires adjuvant metabolic effectors and conceivably, that these effectors are of mitochondrial origin. Ultimately, the metastatic trait in tumor cells may be triggered by a hitherto unknown master switch that would link cytoplasmic and mitochondrial metabolic pathways in such a manner that both, energy and resistance to anoikis would be simultaneously procured. To that effect one must emphasize that mitochondria occupy a central role in both processes.

ACKNOWLEDGMENTS

The authors wish to acknowledge the financial support of CAPES, CNPq, FAPERJ, FAF and INCT/CNPq-Cancer. The authors would like to thank Dr. Antonio Galina and Dr. Marcus Oliveira (Instituto de Bioquimica Médica Leopoldo De Meis, Universidade Federal do Rio de Janeiro) for insightful discussion during the preparation of the manuscript.

REFERENCES

Amoedo ND, Valencia JP, Rodrigues MF, Galina A, Rumjanek FD. 2013. How does the metabolism of tumour cells differ from that of normal cells. Biosci Rep 15:33.

Buchwald M, Kramer OH, Heinzel T. 2009. HDACi–targets beyond chromatin. Cancer Lett 280:160–167.

Choudhary C, Kumar C, Gnad F, Nielsen ML, Rehman M, Walther TC, Olsen JV, Mann M. 2009. Lysine acetylation targets protein complexes and co-regulates major cellular functions. Science 325:834–840.

Chueh Anderly C, Tse Janson WT, Tögel Lars, Mariadason John M. 2014. Mechanisms of histone deacetylase inhibitor-regulated gene expression in cancer cells. Antioxid Redox Signal. doi:10.1089/ars.2014.5863. [Epub ahead of print].

Coller HA. 2014. Is cancer a metabolic disease? Am J Pathol 184:4–17.

Falchook GS, Fu S, Naing A, Hong DS, Hu W, Moulder S, Wheler JJ, Sood AK, Bustinza-Linares E, Parkhurst KL, Kurzrock R. 2013. Methylation and histone deacetylase inhibition in combination with platinum treatment in patients with advanced malignancies. Invest New Drugs 31:1192–1200.

Goncalves P, Martel F. 2013. Butyrate and colorectal cancer: The role of butyrate transport. Curr Drug Metab 14:994–1008.

Grant C, Rahman F, Piekarz R, Peer C, Frye R, Robey RW, Gardner ER, Figg WD, Bates SE. 2010. Romidepsin: A new therapy for cutaneous T-cell lymphoma and a potential therapy for solid tumors. Expert Rev Anticancer Ther 10:997–1008.

Guan KL, Xiong Y. 2011. Regulation of intermediary metabolism by protein acetylation. Trends Biochem Sci 36:108–116.

Hamilton SD, Pardue HL. 1984. Quantitation of lactate by a kinetic method with an extended range of linearity and low dependence on experimental variables. Clin Chem 30:226–229.

Hanahan D, Weinberg RA. 2011. Hallmarks of cancer: The next generation. Cell 144:646–674.

Hitchler MJ, Oberley LW, Domann FE. 2008. Epigenetic silencing of SOD2 by histone modifications in human breast cancer cells. Free Radic Biol Med 45:1573–1580.

Holliday DL, Speirs V. 2011. Choosing the right cell line for breast cancer research. Breast Cancer Res 13:215.

Hutter E, Renner K, Pfister G, Stockl P, Jansen-Durr P, Gnaiger E. 2004. Senescence-associated changes in respiration and oxidative phosphorylation in primary human fibroblasts. Biochem J 380:919-928.

Kaufman JL, Fabre C, Lonial S, Richardson PG. 2013. Histone deacetylase inhibitors in multiple myeloma: Rationale and evidence for their use in combination therapy. Clin Lymphoma Myeloma Leuk 13:370–376.

Kim SC, Sprung R, Chen Y, Xu Y, Ball H, Pei J, Cheng T, Kho Y, Xiao H, Xiao L, Grishin NV, White M, Yang XJ, Zhao Y. 2006. Substrate and functional diversity of lysine acetylation revealed by a proteomics survey. Mol Cell 23:607–618.

Lee JH, Choy ML, Marks PA. 2012. Mechanisms of resistance to histone deacetylase inhibitors. Adv Cancer Res 116:39–86.

Li T, Liu M, Feng X, Wang Z, Das I, Xu Y, Zhou X, Sun Y, Guan KL, Xiong Y, Lei QY. 2014. Glyceraldehyde-3-phosphate dehydrogenase is activated by lysine 254 acetylation in response to glucose signal. J Biol Chem 289:3775–3785.

Livak KJ, Schmittgen TD. 2001. Analysis of relative gene expression data using real-time quantitative PCR and the 2(-Delta Delta C(T)) Method. Methods 25:402–408.

Moreno- Sanchez R, Marin-Hernandez A, Gallardo-Perez JC, Quezada H, Encalada R, Rodriguez-Enriquez S, Saavedra E. 2012. Phosphofructokinase type 1 kinetics, isoform expression, and gene polymorphisms in cancer cells. J Cell Biochem 113:1692–1703.

Moreno- Sanchez R, Marin-Hernandez A, Saavedra E, Pardo JP, Ralph SJ, Rodriguez-Enriquez S. 2014. Who controls the ATP supply in cancer cells? Biochemistry lessons to understand cancer energy metabolism. Int J Biochem Cell Biol 50:10–23.

Mosmann T. 1983. Rapid colorimetric assay for cellular growth and survival: Application to proliferation and cytotoxicity assays. J Immunol Methods 65:55–63.

Mullen AR, Wheaton WW, Jin ES, Chen PH, Sullivan LB, Cheng T, Yang Y, Linehan WM, Chandel NS, DeBerardinis RJ. 2012. Reductive carboxylation supports growth in tumour cells with defective mitochondria. Nature 481:385–388.

Owens KM, Kulawiec M, Desouki MM, Vanniarajan A, Singh KK. 2011. Impaired OXPHOS complex III in breast cancer. PLoS ONE 6:e23846.

Sastre- Serra J, Nadal-Serrano M, Pons DG, Roca P, Oliver J. 2013. The over-expression of ERbeta modifies estradiol effects on mitochondrial dynamics in breast cancer cell line. Int J Biochem Cell Biol 45:1509–1515.

Skehan P, Storeng R, Scudiero D, Monks A, McMahon J, Vistica D, Warren JT, Bokesch H, Kenney S, Boyd MR. 1990. New colorimetric cytotoxicity assay for anticancer-drug screening. J Natl Cancer Inst 82:1107–1112.

Sun S, Han Y, Liu J, Fang Y, Tian Y, Zhou J, Ma D, Wu P. 2014. Trichostatin A targets the mitochondrial respiratory chain, increasing mitochondrial reactive oxygen species production to trigger apoptosis in human breast cancer cells. PLoS ONE 9:e91610.

Ungerstedt JS, Sowa Y, Xu WS, Shao Y, Dokmanovic M, Perez G, Ngo L, Holmgren A, Jiang X, Marks PA. 2005. Role of thioredoxin in the response of normal and transformed cells to histone deacetylase inhibitors. Proc Natl Acad Sci USA 102:673–678.

Wang YP, Zhou LS, Zhao YZ, Wang SW, Chen LL, Liu LX, Ling ZQ, Hu FJ, Sun YP, Zhang JY, Yang C, Yang Y, Xiong Y, Guan KL, Ye D. 2014. Regulation of G6PD acetylation by SIRT2 and KAT9 modulates NADPH homeostasis and cell survival during oxidative stress. EMBO J 33:1304–1320.

Wellen KE, Hatzivassiliou G, Sachdeva UM, Bui TV, Cross JR, Thompson CB. 2009. ATP-citrate lyase links cellular metabolism to histone acetylation. Science 324:1076–1080.

Xu WS, Parmigiani RB, Marks PA. 2007. Histone deacetylase inhibitors: Molecular mechanisms of action. Oncogene 26:5541–5552.

Zaidi N, Swinnen JV, Smans K. 2012. ATP-citrate lyase: A key player in cancer metabolism. Cancer Res 72:3709–3714.

Zhao D, Zou SW, Liu Y, Zhou X, Mo Y, Wang P, Xu YH, Dong B, Xiong Y, Lei QY, Guan KL. 2013. Lysine-5 acetylation negatively regulates lactate dehydrogenase A and is decreased in pancreatic cancer. Cancer Cell 23:464–476.

SUPPORTING INFORMATION

Additional supporting information may be found in the online version of this article at the publisher's web-site.